

This article was downloaded by:

On: 30 January 2011

Access details: *Access Details: Free Access*

Publisher *Taylor & Francis*

Informa Ltd Registered in England and Wales Registered Number: 1072954 Registered office: Mortimer House, 37-41 Mortimer Street, London W1T 3JH, UK



## Spectroscopy Letters

Publication details, including instructions for authors and subscription information:

<http://www.informaworld.com/smpp/title~content=t713597299>

### Relative Quantification of Dynamic Infrared Linear Dichroism Signals and Their Relation to Thermomechanical Properties

Yanqia Wang<sup>a</sup>; Steven R. Aubuchon<sup>b</sup>; Jon R. Schoonover<sup>c</sup>; Richard A. Palmer<sup>a</sup>

<sup>a</sup> Department of Chemistry, Duke University, Durham, North Carolina, USA <sup>b</sup> TA Instruments, New Castle, Delaware, USA <sup>c</sup> Mail Stop E549, Materials Science and Technology Division, Los Alamos National Laboratory, Los Alamos, New Mexico, USA

**To cite this Article** Wang, Yanqia , Aubuchon, Steven R. , Schoonover, Jon R. and Palmer, Richard A.(2005) 'Relative Quantification of Dynamic Infrared Linear Dichroism Signals and Their Relation to Thermomechanical Properties', *Spectroscopy Letters*, 38: 6, 809 — 824

**To link to this Article: DOI:** 10.1080/00387010500316155

**URL:** <http://dx.doi.org/10.1080/00387010500316155>

### PLEASE SCROLL DOWN FOR ARTICLE

Full terms and conditions of use: <http://www.informaworld.com/terms-and-conditions-of-access.pdf>

This article may be used for research, teaching and private study purposes. Any substantial or systematic reproduction, re-distribution, re-selling, loan or sub-licensing, systematic supply or distribution in any form to anyone is expressly forbidden.

The publisher does not give any warranty express or implied or make any representation that the contents will be complete or accurate or up to date. The accuracy of any instructions, formulae and drug doses should be independently verified with primary sources. The publisher shall not be liable for any loss, actions, claims, proceedings, demand or costs or damages whatsoever or howsoever caused arising directly or indirectly in connection with or arising out of the use of this material.

## Relative Quantification of Dynamic Infrared Linear Dichroism Signals and Their Relation to Thermomechanical Properties

**Yanqia Wang**

Department of Chemistry, Duke University, Durham,  
North Carolina, USA

**Steven R. Aubuchon**

TA Instruments, New Castle, Delaware, USA

**Jon R. Schoonover**

Materials Science and Technology Division, Los Alamos National  
Laboratory, Los Alamos, New Mexico, USA

**Richard A. Palmer**

Department of Chemistry, Duke University, Durham,  
North Carolina, USA

**Abstract:** Multivariate curve resolution (MCR) combined with alternating least squares (ALS) has been applied to dynamic infrared linear dichroism (DIRLD) spectra to provide relative quantification and relate this information to the thermomechanical properties of a poly(ester urethane). MCR-ALS analysis reduces the DIRLD data matrix to submatrices of factors and scores. The factors represent spectra-like variables that relate to the DIRLD spectra of the major components constituting the individual DIRLD spectra in the data matrix. The scores are related to the concentration of these factors, and serve as a method to semiquantify the

Received 12 June 2004, Accepted 27 January 2005

This paper was by special invitation as a contribution to a special issue of the journal entitled “Quantitative Vibrational Spectrometry in the 21st Century.” This special issue was organized by Professor Miguel de la Guardia, Professor of Analytical Chemistry at Valencia University, Spain.

Address correspondence to Jon R. Schoonover, Mail Stop E549, Materials Science and Technology Division, Los Alamos National Laboratory, Los Alamos, NM 87545, USA. E-mail: schoons@lanl.gov

components that represent the primary molecular-level mechanisms in the dynamic mechanical temperature scan.

**Keywords:** Dynamic infrared linear dichroism, multivariate curve resolution, poly(ester urethane)

## INTRODUCTION

Multivariate curve resolution–alternating least squares (MCR-ALS) analysis is a chemometric tool that has proved to be valuable in a variety of applications including spectroscopic chemical imaging and vibrational spectroscopy studies.<sup>[1–3]</sup> In the analysis of vibrational spectroscopy data sets, this approach uses an initial step to generate abstract factors and scores; these initial estimates are then refined in a second step into spectra of the pure components and concentration-related scores. This second step uses an iterative alternating least squares optimization of the factor and score matrices. In the current analysis, MCR-ALS provides semiquantitative analysis of the dynamic infrared linear dichroism (DIRLD) signals from a simultaneous dynamic mechanical analysis/dynamic infrared linear dichroism (DMA/DIRLD) experiment.

DIRLD is a rheo-optical technique in which infrared dichroism measurements are combined with a dynamic mechanical perturbation. The dynamic perturbation in this study is sinusoidal tensile deformation. Infrared dichroism uses polarized radiation to probe molecular-level anisotropy of oriented systems, and the DIRLD signals can reveal the different responses of functional groups in the dynamic mechanical process.<sup>[4–7]</sup> Dynamic mechanical analysis (DMA) is a rheological technique that probes the macroscopic viscoelastic properties of materials with a small repetitive deformation. In the current experiments, DIRLD is used as a combination of Fourier-transform infrared linear dichroism spectroscopy and DMA. The goal of this study is to monitor the reorientation of electric dipole-transition moments associated with the vibrations of different functional groups caused by the small-amplitude mechanical oscillation and as a function of temperature in the DMA temperature scan.

The temperature dependence of the properties of polymeric materials is important because large changes in mechanical properties can accompany changes in temperature. As the temperature is raised, a transition in the polymer from a glassy to a rubbery state occurs.<sup>[8]</sup> In viscoelastic polymers, like poly(ester urethanes), the glass transition is associated with a change in free volume and large changes in mechanical properties.<sup>[9]</sup> In the glassy state at lower temperatures, as the polymer is deformed, stored elastic energy relates to small displacements of functional groups in the polymer. As the temperature is raised and the rubbery state is reached, elastic deformations are associated with changes in molecular conformations.

## EXPERIMENTAL

### Materials

The polymer of interest in this study is Estane 5703 (B.F. Goodrich, Charlotte, NC) poly-(butylene adipate)-poly(4,4'diphenylmethane diisocyanate-1,4 butanediol; hereafter referred to as Estane). Thin films of Estane were prepared by solvent casting, as described previously.<sup>[10]</sup> The DIRLD measurements were performed on rectangular pieces of Estane films mounted between the tensile mode clamps of the DMA instrument. The initial dimensions of the film between the clamps were approximately 3.0 by 10.0 mm and 0.02-mm thick. The sample was then stretched four or five times its normal length to introduce molecular orientation in the film. In addition to pure Estane samples, two samples with differing amounts added plasticizer were analyzed. Added plasticizer changes the glass transition temperature and affects the mechanical behavior of the polymer. The plasticizer in these studies is commonly referred to as nitroplasticizer and is a 50/50 by weight mixture of bis(2,2'-dinitropropyl)formal and bis(2,2'-dinitropropyl)acetal.

### Methods

The DIRLD measurements were performed with a Bruker Optics (Billerica, MA) IFS66/s FTIR spectrometer equipped with an external liquid N<sub>2</sub>-cooled mercury-cadmium-telluride (MCT) detector. The spectrometer was operated in step-scan mode with two external digital LIAs (Stanford Research Systems, Sunnyvale, CA, Model SRS850) used for phase and signal demodulation. The DMA used in this study was a Thermal Analysis Q-800 (TA Instruments, New Castle, DE); modified in order to interface it to the FTIR bench.<sup>[11]</sup>

The DMA-controlled step increment was used for temperature scanning. The temperature was ramped from -50°C to +30°C with steps of 1.0°C near the glass transition temperature (T<sub>g</sub>). In the region below -20.0°C and above +20.0°C, larger steps of 2.0°C were used. At each temperature, the equilibrating time was adjusted to synchronize measurements with the step-scan instrument. The mechanical response of the sample and auxiliary signals were collected simultaneously with the step-scan FTIR DIRLD data. Identical temperature scans were repeated on the same sample at both parallel and perpendicular IR polarizations, as previously described.<sup>[9-12]</sup>

A 20 Hz sinusoidal, 0.5% strain modulation was employed on the Estane film samples without added plasticizer. For the plasticized Estane, lower static force and smaller amplitude (0.3%) strains were employed. The FTIR spectra were collected with an 8 cm<sup>-1</sup> spectral resolution and an undersampling ratio of 16.

### MCR Analysis

In the MCR-ALS analysis, an individual DIRLD spectrum,  $D$ , in the matrix of DIRLD spectra as a function of temperature, can be considered as the sum of the individual spectra of the different pure components in the system. In this study, the pure component spectra will be related to the dynamic responses and their variation with temperature.

$$D = \sum_{k=1}^p S_k C_k \quad (1)$$

For the matrix of DIRLD spectra,  $p$  is the number of responses, or processes, that contribute to the observed infrared absorbance in  $D$ .  $S_k$  is the spectrum representing the particular process  $k$ , while  $C_k$  is the prevalence, or concentration, of the particular process.  $C_k$ , therefore, represents the relative quantification of the process for each spectrum in the series.

For a series of  $n$  DIRLD spectra measured as a function of temperature,

$$D_j = \sum_{k=1}^p S_k C_{kj} \quad \text{for } j = 1, 2, \dots, n \quad (2)$$

where  $C_{kj}$  is the coefficient representing the relative amount of spectrum  $S_k$  in the  $j$ th sample. Each  $D_j$  then contains the relative quantitation of the spectrum of sample  $j$  at  $m$  spectral resolution elements (or as a function of DIRLD wavenumber, which correlates the number of data points in the spectrum). If each  $D_j$  is placed as a column in a matrix, the entire DIRLD data set of  $n$  spectra can be expressed in a matrix,  $\mathbf{D}$ , of dimension  $m$  by  $n$ . The two-dimensional data arrays that were analyzed consisted of 63 spectra measured in the temperature range  $-50^\circ\text{C}$  to  $30^\circ\text{C}$  and a wavenumber range of  $1800$  to  $1000\text{ cm}^{-1}$ . The 63 (columns) by 829 (rows) array was analyzed by column. Multiple temperature scans (seven) were performed, analyzed separately, and compared.

$$D_{ji} = \sum_{k=1}^p S_{ik} C_{kj} \quad \text{for } i = 1, 2, \dots, m \quad \text{and } j = 1, 2, \dots, n \quad (3)$$

In matrix notation, this equation becomes

$$\mathbf{D} = \mathbf{SC} \quad (4)$$

where  $\mathbf{D}$ ,  $\mathbf{S}$ , and  $\mathbf{C}$  are matrices of dimension  $m \times n$ ,  $m \times p$ , and  $p \times n$ , respectively. This model represents a generalized Beer's law. This equation can be rearranged and solved for  $\mathbf{S}$  and  $\mathbf{C}$ .

$$\mathbf{S} = (\mathbf{DC}^T)(\mathbf{CC}^T)^{-1} \quad (4a)$$

$$\mathbf{C} = (\mathbf{S}^T \mathbf{S})^{-1} (\mathbf{S}^T \mathbf{D}) \quad (4b)$$

The objective of the MCR-ALS analysis is to solve for **S** and **C**, where **S** represents the DIRLD spectrum of a single process or component (this variable is referred to as a factor in this study), and **C** represents the relative amount of these spectra (these concentration-like variables are referred to as scores).<sup>[13]</sup> In the analysis, **D** can be reconstructed from the product of **C** and **S** plus **E**, which is a matrix of residual contributions unexplained by the extracted factors. If the analysis works properly, **E** is related to noise in the spectra of **D**.

$$\mathbf{D} = \mathbf{SC} + \mathbf{E} \quad (5)$$

The aim of the MCR-ALS application to DIRLD data files is to first resolve the data into pure components that will represent the physical mechanisms occurring, and secondly to determine if the concentration profiles of these components or factors relate to the modulus data. The number of physical components is unknown and correctly estimating the number is essential for adequate resolution of the data set. Before undertaking the MCR-ALS analysis, an estimate of the number of different components associated with the chemical changes in **D** must be determined. This variable is referred to as the chemical rank and is the number of factors contributing to the DIRLD response in the data matrix. In the current work, principle component analysis (PCA) and evolving factor analysis were used to estimate the rank of **D**. The in-phase and quadrature DIRLD spectra were merged into a single data set for analysis. Initial estimations for **C** and **S** are also needed to begin the analysis. Initial estimates can be obtained from evolutionary methods (evolving factor analysis), but pure variable (column or row) methods have used for the initial estimates in the current study. Constraints on the analysis can often assist during the iterative optimization. DIRLD spectra are difference spectra, so the constraint of non-negativity cannot be applied to the factors. However, non-negativity can be applied to the scores. This constraint was the only user applied constraint and was applied with a tolerance up to 5%.

For the optimization step, the default number of iterations in the optimization was 50, and no normalizations were applied during optimization. The MCR-ALS analyses were performed with MATLAB (version 6.5) using a set of programs, written by Prof. R. Tauler and available at <http://www.ub.es/gesq/mcr/mcr.htm>. The optimized pure component spectra (referred to as factor 1 and 2) compromised 99% of the total intensity of the DIRLD spectra at each temperature. The noise level for the in-phase spectra was about 1%, and factors other than the two main factors were below this level and considered noise. The main check for the validity of the factors in this experiment is whether the factors make sense in terms of the chemistry of the system and the accompanying mechanical and temperature perturbations of the system.

The storage modulus ( $E'$ ) and loss modulus ( $E''$ ) are measured for Estane and shown in Fig. 1. With repetitive stress and strain, the mechanical behavior

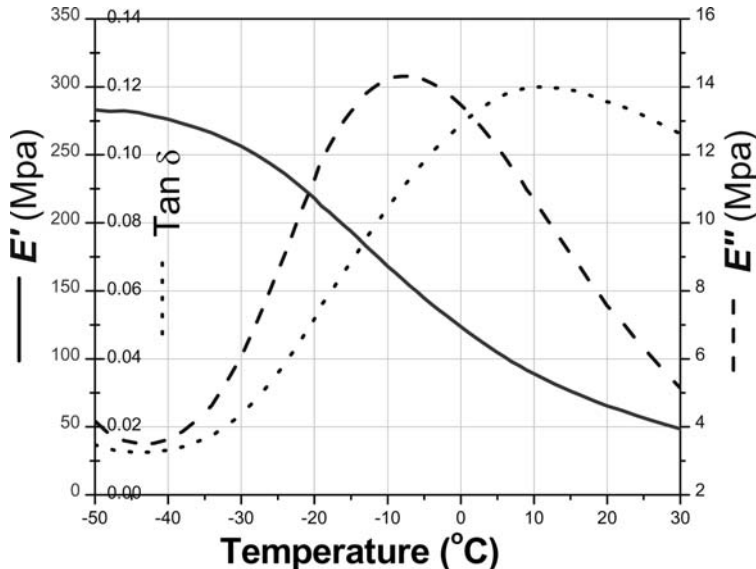


**Figure 1.** The DMA responses as functions of temperature:  $E'$  storage modulus (—),  $E''$  loss modulus (---), and  $\tan \delta$  (· · · · ·).

is referred to as the dynamic mechanical moduli. The storage modulus is a measure of the energy stored elastically during deformation, while the loss modulus is a measure of the energy converted to heat. The MCR-ALS score results were related to this mechanical data. The normalization and rotation of the score values for comparison to the storage modulus ( $E'$ ) and loss modulus ( $E''$ ) were performed separate from the MCR-ALS analysis. A 7-point smoothing was applied to the scores as a function of temperature. Plots were generated with Microcal Origin (version 7.0). The linear combination of the scores for the two factors was used to correlate the modulus curves. The goal is to relate the process that gives rise to the DIRLD signal to the modulus. For the  $E'$  correlation, the initial step was to define a vector ( $V_1$ ) in the form of

$$CP_1 + iCP_2 \quad (6)$$

where  $CP_1$  are the scores for factor 1, while  $CP_2$  are the scores for the factor 2, both from the in-phase DIRLD data. A rotational vector in form of

$$C_1 + iC_2 \quad (7)$$

is defined, where  $C_1$  and  $C_2$  are two real number coefficients. A dot product is applied on the two vectors with the result in form of

$$C_1 * CP_1 + C_2 * CP_2 \quad (8)$$

This equation represents a linear combination of the two sets of scores. The dot product and the  $E'$  curve can then be normalized and displayed. The value of rotational vector is adjusted until the best fit is achieved. The same correlation procedure was also applied for  $E''$  using the DIRLD quadrature data.

## RESULTS AND DISCUSSION

For the multivariate curve resolution analysis, the aim is to recover the DIRLD response profiles of the individual processes as the temperature is raised and repetitive tensile deformation applied. No prior information is available for how the DIRLD signal should change through the DMA scan or how many different processes this signal represents. The goal of this analysis is to identify the individual components or processes and recover semi-quantitative information for these processes. These results can further be related to the DMA results, providing a correlation between the DIRLD results and the thermomechanical data, in effect, between the microscopic (molecular and sub-molecular) and the macroscopic rheology.

From the DMA experiment, the storage modulus ( $E'$ ), loss modulus ( $E''$ ), and  $\tan \delta$  ( $\tan \delta = E''/E'$ ) are plotted as a function of temperature in Fig. 1. The storage modulus monotonically decreases with increasing temperature, the loss modulus reveals a clear  $\alpha$  transition ( $T_g$ ) centered near  $-10^\circ\text{C}$ , and the  $\tan \delta$  shows a distinct transition near about  $+10^\circ\text{C}$ .

The static infrared absorbance spectrum and in-phase and quadrature DIRLD difference spectra of Estane in the  $-50^\circ\text{C}$  to  $+30^\circ\text{C}$  temperature range are shown in Fig. 2. The major absorbance features in the static spectrum of Estane are mirrored in the DIRLD spectra. The infrared bands for the static spectrum are assigned in Table 1 with segment origin (hard or soft), along with the major vibration constituting the normal mode. The DIRLD spectra are consistent with the previous results.<sup>[9–12]</sup> In the DIRLD data, the functional groups that align with the stretch direction demonstrate positive bands in the difference spectra, with negative bands evident for functional groups reorienting away from the stretch direction.

The DIRLD spectra resolve the highly overlapped features based on the difference in reorientation rates, directions, and susceptibilities of the functional groups.<sup>[4–7]</sup> The carbonyl region of the spectrum is especially complex with different types of carbonyls as well as hydrogen-bonding and non-hydrogen-bonding interactions. The sign of the carbonyl absorption band is negative in both the in-phase and quadrature spectra, indicating, as expected, that the overall dipole-transition moments for the carbonyl groups are reorienting perpendicularly to the direction of the applied strain.<sup>[10]</sup> The negative features from 1500 to  $1000\text{ cm}^{-1}$  are primarily associated with the bisignate bands from vibrations of polymer backbone functional groups. The bisignate features are believed to be caused by the band position shifts and shape changes rather than solely dipole reorientations.<sup>[10,12]</sup> Some

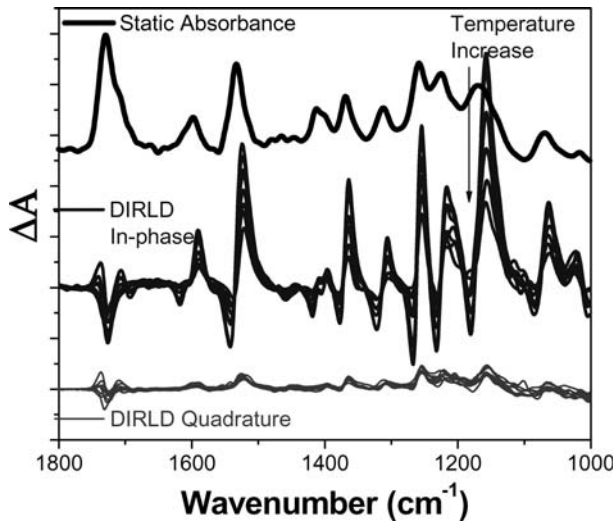


**Figure 2.** The static FTIR absorbance spectrum DIRLD (top), the in-phase DIRLD spectra (middle), and the quadrature DIRLD spectra (bottom).

**Table 1.** Static infrared assignments for estane (1800–1000 cm<sup>−1</sup>)

cm <sup>−1</sup>	Assignment	Domain origin
1732	$\nu(\text{C}=\text{O})$	Hard/soft
1612	Phenyl ring mode, primarily $\nu(\text{C}=\text{C})$	Hard
1597	Phenyl ring mode, primarily $\nu(\text{C}=\text{C})$	Hard
1533	$\nu(\text{C}=\text{N}) + \delta(\text{NH})$	Hard
1478	$\delta(\text{CH}_2)$	Hard/soft
1463	$\delta(\text{CH}_2)$	Soft
1436	$\delta(\text{CH}_2)$	Soft
1415	Phenyl ring mode, primarily $\nu(\text{C}-\text{C})$	Hard
1395	w(CH <sub>2</sub> )	Soft
1362	w(CH <sub>2</sub> )	Soft
1319	Phenyl ring mode, primarily $\beta(\text{CH})$	Hard
1311	$\nu(\text{C}=\text{N}) + \delta(\text{NH})$	Hard
1254	$\nu(\text{C}-\text{O}-\text{C})$ ; w(CH <sub>2</sub> )	Soft
1223	$\nu(\text{C}=\text{N}) + \delta(\text{NH})$	Hard
1207	Phenyl ring mode	Hard
1176	$\nu(\text{C}-\text{O}-\text{C})$	Soft
1077	$\nu(\text{C}-\text{O}-\text{C})$	Hard/soft
1060	$\nu(\text{C}-\text{O}-\text{C})$	Hard
1018	Phenyl ring mode, primarily $\beta(\text{C}-\text{H})$	Hard

of the bisignate bands may be due to hydrogen-bonding pairs where different reorientation responses are observed for hydrogen-bonded functional groups versus chemically equivalent groups not involved in hydrogen bonding.

Throughout the temperature range, the fundamental features of the in-phase and quadrature spectra are similar. The spectral responses are predominantly in-phase with the mechanical modulation. With the exception of the carbonyl bands, the integral intensities of the DIRLD bands tend to decrease with increasing temperature. The higher mobility of molecular chains at higher temperatures is expected to decrease the DIRLD signal since less orientation occurs. The temperature dependence of the carbonyl groups is complex. The changing pattern for the response of carbonyl groups is a product of different chemical and hydrogen-bonding interactions.

To gain further insight into the DIRLD signal and correlate these data to the DMA results, MCR-ALS analysis was performed on the in-phase and quadrature spectra. The analysis of pure Estane provides a two-factor solution for the combined data set of in-phase and quadrature spectra. The correspondence between multiple data sets was excellent, particularly for the in-phase data. The correspondence between quadrature data in different experiments was poor due to the low quadrature signal.

The two factors are shown in Fig. 3, and the assignments for the DIRLD features of the two factors are listed in Table 2. At all the temperatures, these two factors constitute over 99% of the total absorbance values. Factor 1 shows several bisignate bands and higher absorbance values compared to factor 2. The bands in factor 1 show more structure such as the splitting of the carbonyl band (1735 and 1713  $\text{cm}^{-1}$ ) and a shoulder of the  $\nu(\text{CN}) + \delta(\text{NH})$

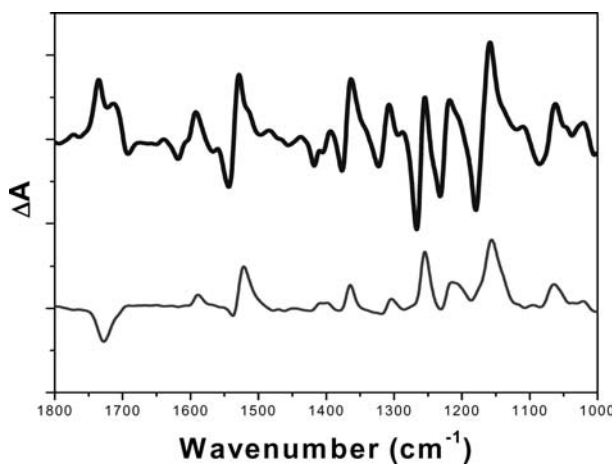


**Figure 3.** The two extracted factors from the MCR-ALS analysis of the DIRLD spectra of pure Estane from  $-50^\circ\text{C}$  to  $+30^\circ\text{C}$ .

**Table 2.** Assignment of DIRLD features from MCR-ALS analysis

Factor 1	Factor 2	Orientation	Assignments
1735			$\nu(C=O)$ non-hydrogen-bonded, ester or urethane
	1728	$\perp$	$\nu(C=O)$ hydrogen-bonded, ester
1714			$\nu(C=O)$ hydrogen-bonded, urethane
1610		$\perp$	Phenyl ring, urethane, primarily $\nu(C=C)$
1592	1589		Phenyl ring, urethane (primarily $\nu(C=C) + \delta(N-H)$ )
1420		$\perp$	Phenyl ring, urethane
	1415		Phenyl ring, urethane
1394	1399		$CH_2$ wag, ester
1380/1364		Bisignate	$CH_2$ wag, ester
	1364		$CH_2$ wag, ester
1316/1307		Bisignate	$\nu(C-N) + \delta(N-H)$ , urethane
	1304		$\nu(C-N) + \delta(N-H)$ , urethane
1265/1255		Bisignate	$\nu(C-O-C)$ ; $(CH_2)$ wag, ester
	1255		$\nu(C-O-C)$ ; $(CH_2)$ wag, ester
1229/1218		Bisignate	$\nu(C-N) + \delta(N-H)$ , urethane
	1215		$\nu(C-N) + \delta(N-H)$ , urethane
1170/1159		Bisignate	$\nu(C-O-C)$ , ester
	1156		$\nu(C-O-C)$ , ester
1080/1062		Bisignate	$\nu(C-O-C)$ , ester and urethane
	1064		$\nu(C-O-C)$ , ester and urethane
	1019		Phenyl ring, urethane

DIRLD, dynamic infrared linear dichorism; MCR-ALS, multivariate curve resolution-alternating least squares.

band near  $1525\text{ cm}^{-1}$ . The carbonyl bands present in the two factors possess different reorientation directions. The carbonyl bands in factor **1** exhibit the same sign (positive) as the bands of the polymer backbone, whereas those of factor **2** are negative.

The MCR-ALS analysis is able to extract the differing carbonyl contributions. In factor **1**, the carbonyl bands exhibit the same sign as the backbone bands, which indicates that carbonyl groups are reorienting in the strain direction. For factor **2**, the  $C=O$  groups show the opposite sign from the backbone groups, indicating reorientation away from the strain direction. In the simplest model, the  $C=O$  groups are all expected to reorient perpendicular to the backbone groups.<sup>[9–12]</sup> However, the DIRLD experiment is able to differentiate the different types of carbonyl groups in the polymer. Two basic types of carbonyl groups are those identified from the urethane (hard) segments and those from the ester (soft) segments. More subtle environmental differences that are possible include ester carbonyl

groups or urethane carbonyl groups at the interface of the two domains, urethane carbonyl groups within a soft domain, or ester carbonyl groups within a hard domain. In addition, these various types of carbonyls can also have different orientations and hydrogen-bonding interactions within the polymer. Even though all carbonyl groups follow the same reorientation mechanism by rotating away from the polymer backbone, the backbone orientation can be different from the strain direction for some number of carbonyl groups. In this experiment the polymer is not perfectly aligned, so the reorientation direction will not be the same for all parts of the polymer.

The abundance of bisignate bands and stronger spectral intensity in factor **1** indicates that the primary processes represented by factor **1** are small shifts in band position accompanied by reorientation effects. On the other hand, the spectra for factor **2** can be interpreted as due almost exclusively to reorientation effects.

Figure 4 shows the scores for the two extracted factors from the in-phase spectra. The MCR-ALS analysis provides relative quantification of spectral absorbance with the score plots of the two extracted factors, representing their contributions to the total spectral absorbance. The scores provide the contribution of the two factors for each individual DIRLD spectrum. The scores of both factors decrease monotonically with increasing temperature. In addition, the scores of factor **1** decrease less than factor **2** in the  $-50^{\circ}\text{C}$  to  $-20^{\circ}\text{C}$  region. In contrast to the in-phase data, the score plots for the quadrature data show clear inflections. The quadrature signal (Fig. 4) is much weaker than the in-phase signal, but the scores do demonstrate maxima near  $-15^{\circ}\text{C}$ , which is close to the  $T_g$  ( $\sim -10^{\circ}\text{C}$ ) determined from the DMA measurements.

The in-phase and quadrature DIRLD signals relate to the spectral responses in-phase with, and  $90^{\circ}$  out-of-phase with, the strain perturbation. At the same time, the storage modulus ( $E'$ ) and loss modulus ( $E''$ ) are the mechanical responses in-phase with, and  $90^{\circ}$  out-of-phase, with the strain perturbation. This parallel relationship suggests a correlation between the macroscopic thermomechanical behavior and the molecular-level spectral behavior. The best correlations with  $E'$  and  $E''$  using these scores are shown in Fig. 5. The in-phase scores compared to the  $E'$  curve from the DMA measurements demonstrate a correlation throughout the temperature range. The curve of the out-of-phase scores compared to the  $E''$  curve shows inflections near  $T_g$ , but the correlation is not as good as the in-phase relation, likely due to the much weaker quadrature signal. The low quadrature signal precludes any meaningful correlation between the scores and  $E''$ .

To further test the validity of these correlations, samples of Estane with 10% and 30% (by weight) added plasticizer were studied in the same manner as pure Estane. For Estane with 30% added plasticizer, the MCR-ALS analysis extracts two factors very similar to those extracted for pure Estane. The plasticization of Estane shifts the  $\alpha$  transition to lower temperature. The  $E'$  correlation using the scores of these two factors demonstrates

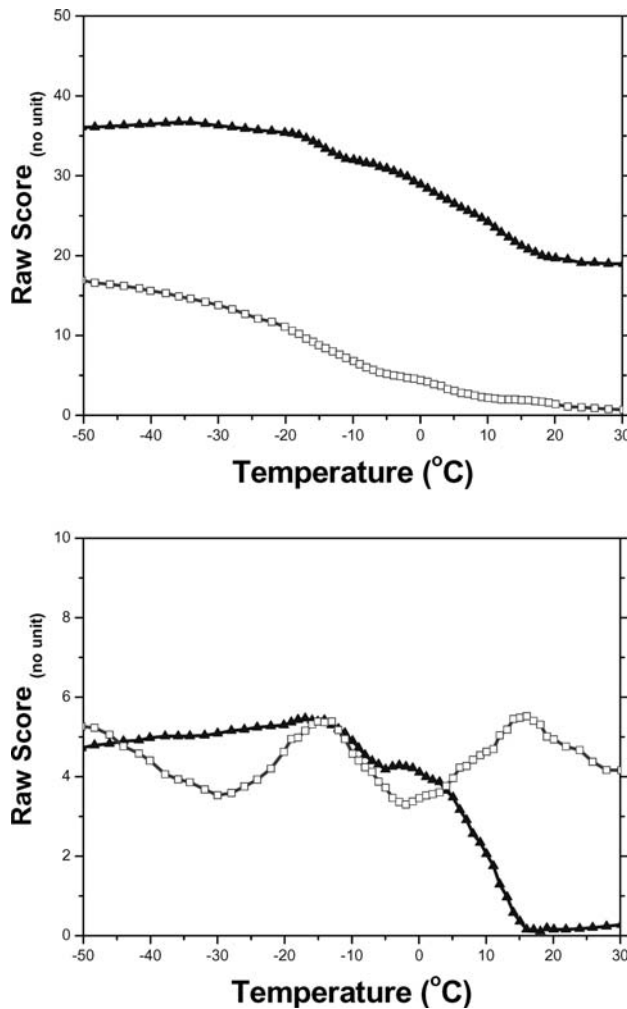


**Figure 4.** The scores for the two factors for the in-phase DIRLD spectra (top) and the quadrature spectra (bottom).

this shift showing that the DIRLD experiment is tracking the changes in the temperature-dependent mechanical properties of Estane. The modulus correlation is shown in Fig. 6. The correlation in the top panel of Fig. 6 shows that the score correlate with  $E'$ . Both of these plots demonstrate a steeper slope centered at about  $-20^{\circ}\text{C}$ , whereas without added plasticizer a more gradual slope is evident centered near  $-10^{\circ}\text{C}$  (top panel of Fig. 5). This same trends was found for experiments on Estane with 10% plasticizer.

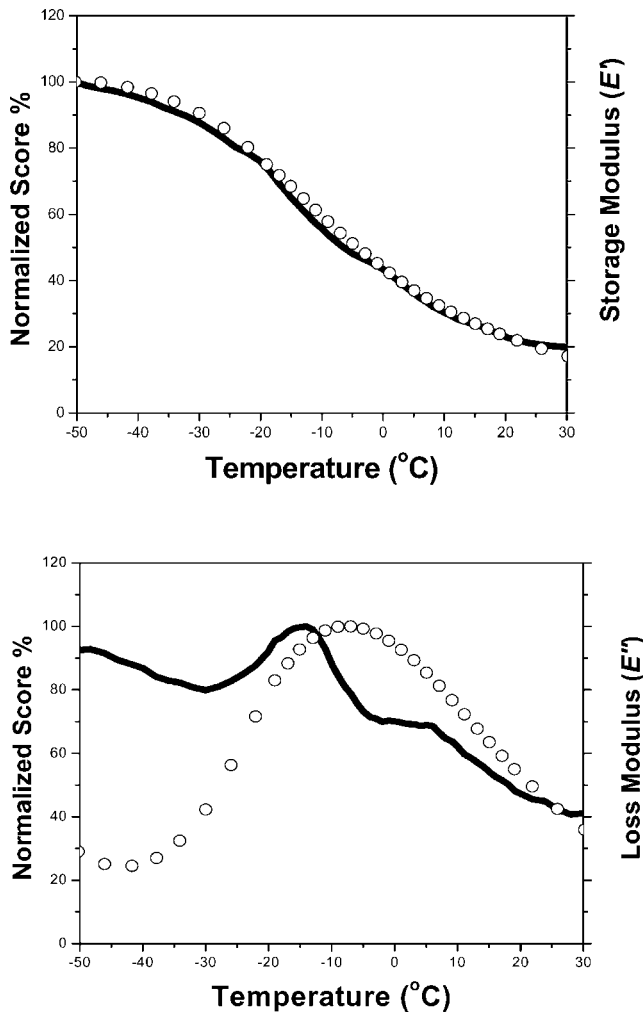


**Figure 5.** Modulus correlation of the MCR-ALS scores of the in-phase DIRLD data with  $E'$  and of the quadrature DIRLD data with  $E''$  for pure Estane.

## CONCLUSIONS

This work represents a unique example of using MCR-ALS analysis to interpret DIRLD data and extract the primary physical mechanisms occurring in the DMA experiment. MCR-ALS is typically applied to data sets to extract pure components of samples such as mixtures. In the current study, two components or factors are extracted, their concentration profile or scores used as a relative quantification of these two factors, and these scores related to the dynamic mechanical moduli results.

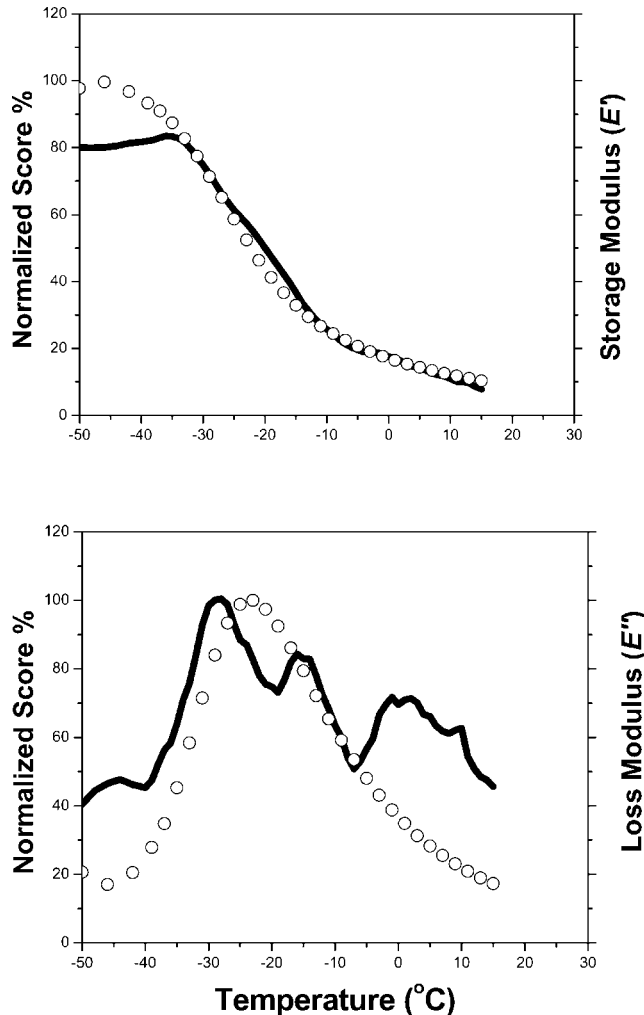


**Figure 6.** Modulus correlation of the MCR-ALS scores of the in-phase DIRLD data with  $E'$  and of the quadrature DIRLD data with  $E''$  for Estane with 30% nitroplasticizer.

Physical interpretations can be forwarded for the two extracted factors. The primary molecular mechanism represented by factor **1** involves the polymer backbone and slippage of chains. In the glassy state at low temperatures, the slight shifts upon tensile perturbation are consistent with the stiffness of the material and are associated with molecular displacements of the polymer backbones of both segments. In the rubbery state, the molecular chains have considerable flexibility to adopt different conformations, and as the temperature is raised, the scores of factor **1** decrease, consistent with fewer interactions

between the chains, less reorientation, and more free volume. The other conformational change evident from factor **1** relates to the parallel reorientation carbonyl groups from the urethane segments. These carbonyl features are related to the hydrogen-bonded and the non-hydrogen-bonded components.

Factor **2** shows features at nearly the same wavenumbers as for factor **1**, but with no bisignate bands. The scores for factor **2** are less than those of factor **1**, and nearly all the bands are positive, indicating primarily reorientation toward the stretching axis. The factor does demonstrate the perpendicular orientation of the hydrogen-bonded ester carbonyl. The best interpretation of factor **2** is that it represents primarily orientation of the polymer with the deformation. The semiquantitative scores of these two factors are used to interpret the DIRLD data, then further correlated with the DMA data.

## ACKNOWLEDGMENTS

The authors gratefully acknowledge the assistance of The Lord Foundation of North Carolina, Bruker Optics, TA Instruments, and Duke University for support of this work. Part of this work was performed at Los Alamos National Laboratory, operated by the University of California for the U.S. Department of Energy under contract number W-7405-ENG-36. Acknowledgment is also made to Dr. R. Tauler and Dr. A. de Juan from the University of Barcelona for assistance with the MCR-ALS analysis.

## REFERENCES

1. Tauler, R.; Kowalski, B.; Fleming, S. Multivariate curve resolution applied to spectral data from multiple runs of an industrial-process. *Anal. Chem.* **1993**, *65*, 2040–2047.
2. Tauler, R. Multivariate curve resolution applied to second order data. *Chemometrics and Intelligent Laboratory Systems* **1995**, *30*, 133–146.
3. Schoonover, J. R.; Marx, R.; Zhang, S. L. Multivariate curve resolution in the analysis of vibrational spectroscopy data files. *Appl. Spectrosc.* **2003**, *57*, 154A–170A.
4. Noda, I.; Dowrey, A. E.; Marcott, C. Dynamic infrared linear dichroism study of high-density and low-density polyethylene near the beta-transition temperature. *J. Mol. Struct.* **1990**, *224*, 265–270.
5. Noda, I.; Dowrey, A. E.; Marcott, C. Characterization of polymers using polarization-modulation infrared techniques: dynamic infrared linear dichroism (DIRLD) spectroscopy. In *Fourier Transform Infrared Characterization of Polymers*; Polymer Science and Technology; Ishida, H., Ed.; Plenum: New York, 1987; Vol. 36, pp. 33–59.
6. Noda, I.; Dowrey, A. E.; Marcott, C. Dynamic infrared linear dichroism of polymer films under oscillatory deformation. *J. Poly. Sci. Poly. Lett.* **1983**, *21*, 99–103.

7. Noda, I.; Dowrey, A. E.; Marcott, C. A spectrometer for measuring time-resolved infrared linear dichroism induced by a small-amplitude oscillatory strain. *Appl. Spectrosc.* **1988**, *42*, 203–216.
8. Ferry, J. S. *Viscoelastic Properties of Polymers*, 3rd ed., Wiley: New York, 1980.
9. Wang, H.; Aubuchon, S. R.; Thompson, D. G.; Osborn, J. C.; Marsh, A. L.; Nichols, W. R.; Schoonover, J. R.; Palmer, R. A. Temperature-dependent dynamic mechanical analysis-Fourier transform infrared study of a poly(ester urethane) copolymer. *Macromolecules* **2002**, *35*, 8794–8801.
10. Wang, H.; Graff, D. K.; Schoonover, J. R.; Palmer, R. A. Static and dynamic infrared linear dichroic study of a polyester polyurethane copolymer using step-scan FTIR and a photoelastic modulator. *Appl. Spectrosc.* **1999**, *53*, 687–696.
11. Wang, Y.; Aubuchon, S. R.; Smith, M. E.; Schoonover, J. R.; Palmer, R. A. Dynamic infrared linear dichroism study of the temperature dependent, viscoelastic behavior of a poly(ester urethane). *Appl. Spectrosc.* **2004**, *59*, 305–315.
12. Graff, D. K.; Wang, H.; Palmer, R. A.; Schoonover, J. R. Static and dynamic FTIR linear dichroism studies of plasticization effects in a polyurethane elastomer. *Macromolecules* **1999**, *32*, 7147–7155.
13. Tauler, R. Calculation of maximum and minimum band boundaries of feasible solutions for species profiles obtained by multivariate curve resolution. *J. Chemom.* **2001**, *15*, 627–646.